Spectral-Domain Analysis of Coplanar Waveguide Traveling-Wave Electrodes and Their Applications to Ti:LiNbO$_3$ Mach–Zehnder Optical Modulators

Kenji Kawano, Tsutomu Kitoh, Hiromichi Jumonji, Toshinori Nozawa, Mitsuaki Yanagibashi, and Toshio Suzuki

Abstract—**Hybrid-mode and quasi-TEM analyses are carried out for coplanar waveguide traveling-wave electrodes applicable to z-cut Ti:LiNbO$_3$ optical modulators. The analyses are based on the spectral-domain approach. The microwave effective index and the characteristic impedance are clarified, together with the microwave conductor loss. These are incorporated to accurately predict the modulator characteristics. It is shown that these characteristics can be greatly improved by employing a thicker buffer layer. High-speed and low-driving-power Ti:LiNbO$_3$ optical modulators are realized at a 1.52 μm wavelength. Agreement between the calculated and measured results is good.**

I. Introduction

High-speed external optical modulators provide a strong alternative to laser diode direct modulation for the next generation of single-mode transmission systems. Among the external optical modulators, Ti:LiNbO$_3$ optical modulators have demonstrated high potential, as mentioned in [1] and [2]. The important factors for evaluating these optical modulators are the optical 3 dB bandwidth and the driving power. However, these factors have a trade-off relationship with respect to the interaction lengths between microwaves and optical waves. The main restriction to the modulation bandwidth is caused by a mismatch in velocity between these waves as well as the conductor losses of the traveling-wave (TW) electrodes. This implies that the TW electrodes play a very important role in Ti:LiNbO$_3$ optical modulators. To develop new optical modulators that improve the modulation bandwidth and driving voltage, a full knowledge of TW electrodes is indispensable. Thus, analyses of the microwave effective index, the characteristic impedance, and microwave conductor losses and related calculated results for the modulator characteristics are very important.

The present authors have previously advanced z-cut Ti:LiNbO$_3$ optical modulators [3], [4], in which coplanar waveguide (CPW) TW electrodes with a narrow center conductor, a wide gap, and a relatively thick buffer layer were employed. These electrodes are useful not only for realizing efficient interactions between the microwaves and optical waves, but also for providing a good impedance match with the 50 Ω driving circuit and efficient mode conversion from the coaxial connectors to the electrodes.

The characteristics of TW electrodes and modulator performance have been modeled extensively [5]. However, the purpose of this paper is to present more detailed analytical results for the CPW TW electrodes. The analyses are based on the hybrid-mode [6] and quasi-TEM [4] spectral-domain approach (SDA). Since LiNbO$_3$ substrates have a strong anisotropic nature, the analysis procedure for the anisotropic material [7] was taken into consideration. Section II describes an analytical model for the CPW TW electrodes. Section III discusses the calculation procedure for the figure of merit (ratio of modulation bandwidth to half-wavelength voltage) and Section IV shows detailed calculation results. First, the convergence characteristics, the microwave effective index, and the characteristic impedance are discussed. The effects of the SiO$_2$ buffer layer on modulation bandwidth, driving voltage, and microwave conductor losses are also clarified. It is shown that the SiO$_2$ buffer layer plays an important role in modulator characteristics and that the modulation bandwidth can be greatly improved by using a thick buffer layer. Section V compares the calculated modulator characteristics with those of fabricated modulators at a 1.52 μm wavelength.

II. Analytical Model

Fig. 1 shows a cross-sectional view of the analyzed Mach–Zehnder intensity modulator under consideration. To analyze the structure, the quasi-TEM and hybrid-mode SDA were employed.

Manuscript received October 23, 1989; revised April 15, 1991.

K. Kawano, T. Nozawa, M. Yanagibashi, and T. Suzuki are with the NTT Opto-Electronics Laboratories, Nippon Telegraph and Telephone Corporation, 3-1 Morinosato Wakamiya, Atsugi-shi, Kanagawa Prefecture, 243-01 Japan.

T. Kitoh is with the NTT Opto-Electronics Laboratories, Nippon Telegraph and Telephone Corporation, Tokai-mura, Naka-gun, Ibaraki Prefecture, 319-11 Japan.

H. Jumonji was with the NTT Opto-Electronics Laboratories, Nippon Telegraph and Telephone Corporation, Kanagawa, Japan. He is now with the Optical Research Center, Ricoh Company Ltd., Yokohama, Japan.

IEEE Log Number 9101649.

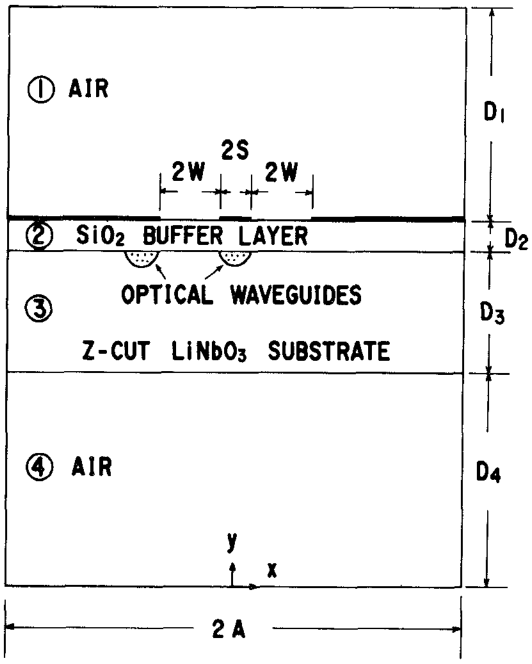

Fig. 1. Cross-sectional view of the analyzed optical modulator.

Although conventional CPW TW electrodes for Ti:$LiNbO_3$ optical modulators have a low characteristic impedance, a wide center conductor, and a narrow gap, the structures shown in these figures have a narrow center conductor and a wide gap to realize efficient interaction between microwaves and optical waves, together with a high characteristic impedance [3], [4], [8]. The center conductor width and gap are $2S$ and $2W$, respectively. The thicknesses of the upper air region, SiO_2 buffer layer, z-cut $LiNbO_3$ substrate, and lower air region are D_1, D_2, D_3, and D_4, respectively. The width of the shielding wall is $2A$. The values for D_1, D_4, and $2A$ are set large enough to simulate an open structure. The thickness (D_3) of the z-cut $LiNbO_3$ substrate is 500 μm. The dielectric constants of the z-cut $LiNbO_3$ substrate are 28 in the y direction and 43 in the x and z directions. The dielectric constant of the SiO_2 buffer layer is 3.9. The electrode thickness is assumed to be zero.

III. Figure of Merit Calculation

To obtain the figure of merit ($\Delta f / V_\pi$), the optical 3 dB modulation bandwidth (Δf) and half-wavelength voltage (V_π) are needed. By employing the SDA, the microwave effective index (n_m), the characteristic impedance (Z), and the microwave conductor loss (α) were calculated. These quantities were incorporated into the modulation bandwidth calculation by using an equivalent circuit model [9], [10]. The half-wavelength voltage was calculated utilizing the overlap integral for the microwave and optical waveguide fields. The calculation procedure for the microwave conductor loss has been discussed by several authors [11]. Here, the following expression was utilized to calculate the conductor loss (α) for the CPW:

$$\alpha = \frac{R_S \int J_s^2 \, dl}{2ZI^2} \tag{1}$$

where J_s is the surface current density, R_s is the surface resistance, Z is the characteristic impedance, and I is the total current density.

Based on this calculation procedure, we developed a computer program which can automatically calculate n_m, Z, α, Δf, V_π, and $\Delta f / V_\pi$ for a given structure. All of the calculations for both the quasi-TEM and the hybrid-mode analysis were performed with a desktop computer.

IV. Numerical Results

In the following calculation, we employed a combination of trigonometric and Maxwell functions as the basis functions [6]. The operating wavelength was assumed to be 1.52 μm.

Parts (a) and (b) of Fig. 2 show the calculated microwave effective index (n_m) and the characteristic impedance (Z) for the CPW TW electrode as a function of the number of basis functions. Fig. 2(a) corresponds to the quasi-TEM upper bound calculation [4]. On the other hand, Fig. 2(b) depicts the calculated results for the hybrid-mode analysis. For both calculations, the center conductor width ($2S$) and gap ($2W$) are assumed to be 8 and 15 μm. For the hybrid-mode analysis, the number of basis functions means the sum of the number of basis functions in the x (M_x) and z (M_z) directions, where M_x is assumed to equal to M_z. In one basis function case, only an x-directed electric field was assumed ($M_x = 1$ and $M_z = 0$). As shown in these figures, the solutions converge as the number of basis functions increases. The convergence characteristics depend heavily on the existence of a buffer layer. Two basis functions for the quasi-TEM analysis and two sets of basis functions ($M_x = M_z = 2$) for the hybrid-mode analysis are sufficient to obtain good convergence when there is no buffer layer. On the other hand, a larger number of basis functions are needed when the buffer layer thickness (D_2) is not equal to zero. Ten basis functions for the quasi-TEM analysis and six sets of basis functions ($M_x = M_z = 6$) for the hybrid-mode analysis were employed to obtain sufficiently converged solutions in the following calculations.

Parts (a) and (b) of Fig. 3 show the calculated microwave effective index (n_m) and the characteristic impedance (Z) based on a quasi-TEM analysis as a function of the ratio ($2S/2W$) of center conductor width ($2S$) to gap ($2W$). The buffer layer thickness (D_2) is employed as a parameter. Here, the center conductor width ($2S$) was assumed to be 8 μm. For comparison, calculated results based on the conformal mapping technique (●) [12] are also shown for the case of no buffer layer. As shown in this figure, the two agree well. This chart is very useful for designing CPW TW electrodes. Considering the impedance match between the CPW TW electrode and the external 50 Ω circuit, the characteristic impedance for

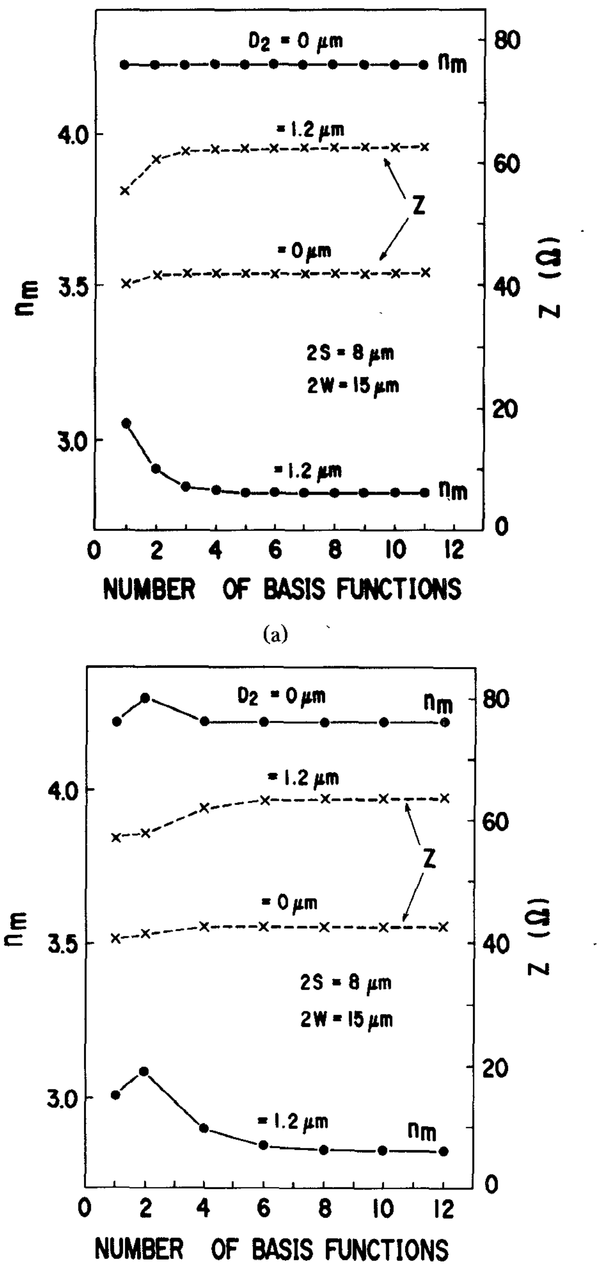

Fig. 2. Calculated microwave effective index (n_m) and characteristic impedance (Z) as a function of the number of basis functions. (a) Quasi-TEM analysis. (b) Hybrid-mode analysis.

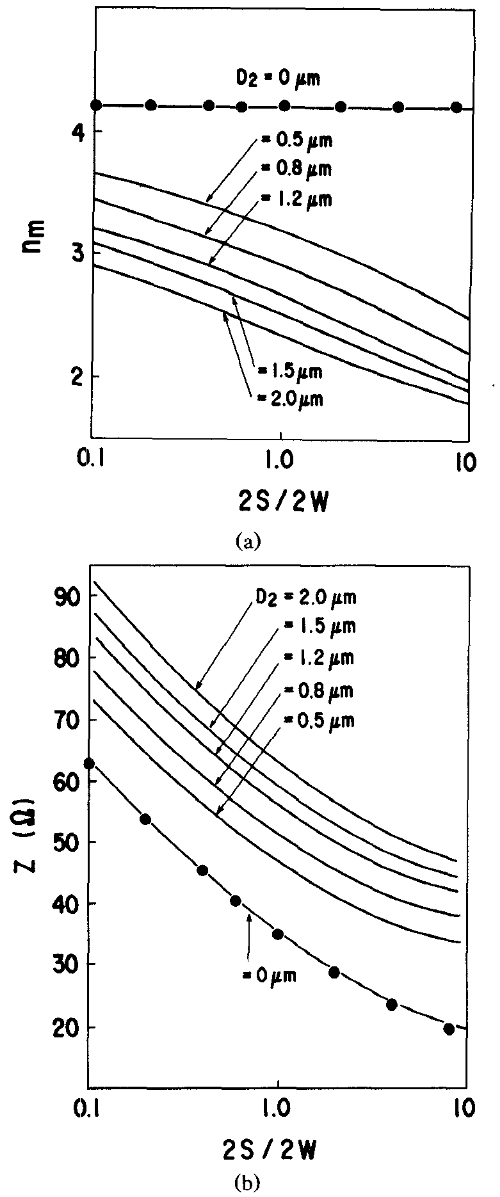

Fig. 3. (a) Calculated microwave effective index (n_m) and (b) characteristic impedance (Z) as a function of the ratio ($2S/2W$) of center conductor width ($2S$) to gap ($2W$). Center conductor width ($2W$) is 8 μm.

the TW electrodes should be set in the range of 40 to 60 Ω. By using Fig. 3, the gap was determined to be 15 μm and $2S/2W$ is 0.53.

Fig. 4 shows the calculated microwave effective index (n_m) and the characteristic impedance (Z) based on a hybrid-mode analysis as a function of frequency. As shown in this figure, there are only a few frequency-dependent characteristics for the interaction part ($2S = 8$ μm and $2W = 15$ μm) owing to their small dimensions. On the other hand, since the dimensions for the segment of the TW electrode that connects the active segment to the coaxial connector (which we call the feedthrough part) are large, frequency-dependent characteristics become significant. In order to clarify the frequency-dependent characteristics, the calculated results for two cases are shown for the feedthrough parts. We can see that the smaller feedthrough part has a smaller frequency dependence. In this study, the center conductor width and the gap for the feedthrough part of the TW electrode were determined to be 300 μm and 700 μm, respectively, for the actual optical modulators that were fabricated.

A hybrid-mode analysis is needed to accurately design the feedthrough parts of a TW electrode. On the other hand, quasi-TEM analysis is sufficient for designing the interaction part. In the following discussions, quasi-TEM analysis was employed to save computer time.

Parts (a) and (b) of Fig. 5 show the calculated microwave effective index (n_m), the characteristic impedance

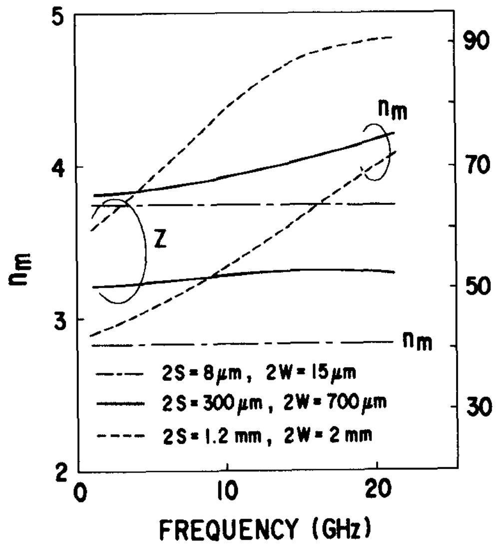

Fig. 4. Calculated microwave effective index (n_m) and characteristic impedance (Z) as a function of frequency.

(Z), and the microwave conductor loss (α) as a function of the buffer layer thickness (D_2). Here, gold was assumed as the conductor. As the buffer layer thickness increases, the microwave effective index decreases and the characteristic impedance increases. It should be noted that the microwave conductor loss (α) can be decreased by a thicker buffer layer.

Fig. 6 shows the calculated results for the product ($\Delta f \cdot L$) of the optical 3 dB modulation bandwidth (Δf) and the interaction length (L) as a function of buffer layer thickness (D_2). Here, only the velocity mismatch between the microwaves and the optical waves was taken into consideration. As shown in this figure, the modulation bandwidth increases as the buffer layer thickness increases.

Fig. 7 shows the calculated results for the product ($V_\pi \cdot L$) of the half-wavelength voltage (V_π) and the interaction length (L) of the microwaves and the optical waves. Here, the FWHM (full width at half maximum) for the optical powers was assumed to be 4.35 μm and 2.85 μm in the x and y directions. These values correspond to optical waveguide fabrication conditions for a Ti thickness of 800 Å and a diffusion conditions of 1000° C, 10 h, and a wet O_2 atmosphere in our laboratory experiments. The product ($V_\pi \cdot L$) increases as the buffer layer thickness, D_2, increases. Here, it should be noted that the important figure of merit for the optical modulators is not $V_\pi \cdot L$ but the ratio ($\Delta f / V_\pi$) of the modulation bandwidth (Δf) to the half-wavelength voltage (V_π). This is because the driving voltage can easily be reduced by lengthening the interaction length (L). In order to realize a driving voltage of less than 5.0 V, the interaction length was determined to be 2.7 cm.

Fig. 8 shows the calculated results for the figure of merit ratio ($\Delta f / V_\pi$) of the modulation bandwidth (Δf) to the half-wavelength voltage (V_π) as a function of the buffer layer thickness (D_2). The effect of the microwave conductor loss is a function of the interaction length (L). As mentioned before, the interaction length was assumed to be 2.7 cm. In this figure, the velocity mismatch between the microwaves and the optical waves and the characteristic impedance mismatch between the TW electrode and the 50 Ω outer circuits, as well as conductor losses, were taken into consideration. The figure of merit ($\Delta f / V_\pi$) is seen to increase as the buffer layer thickness (D_2) increases. The product ($V_\pi \cdot L$) is an almost linear function of the buffer layer thickness. On the other hand, the modulation bandwidth is inversely proportional to the difference between the microwave effective index (n_m) and the optical wave effective index (n_o). As a result, the increase in modulation bandwidth exceeds the increase in half-wavelength voltage. For this reason, an improved figure of merit ($\Delta f / V_\pi$) can be obtained by employing a thicker buffer layer [3], [4], [13]–[16].

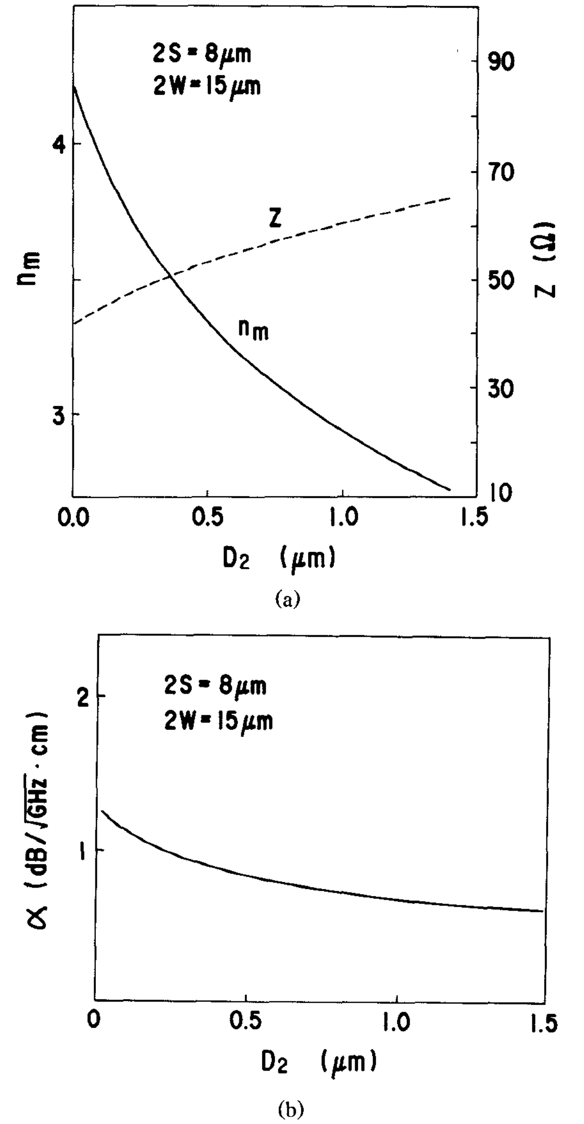

Fig. 5. (a) Calculated microwave effective index (n_m) and characteristic impedance (Z) and (b) microwave conductor loss as a function of buffer layer thickness (D_2).

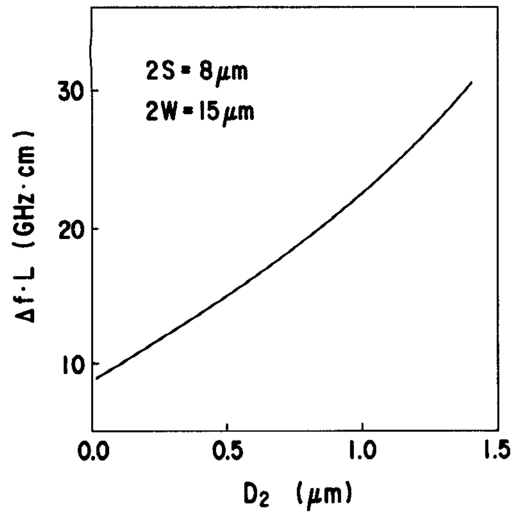

Fig. 6. Calculated optical 3 dB modulation bandwidth (Δf) as a function of buffer layer thickness (D_2).

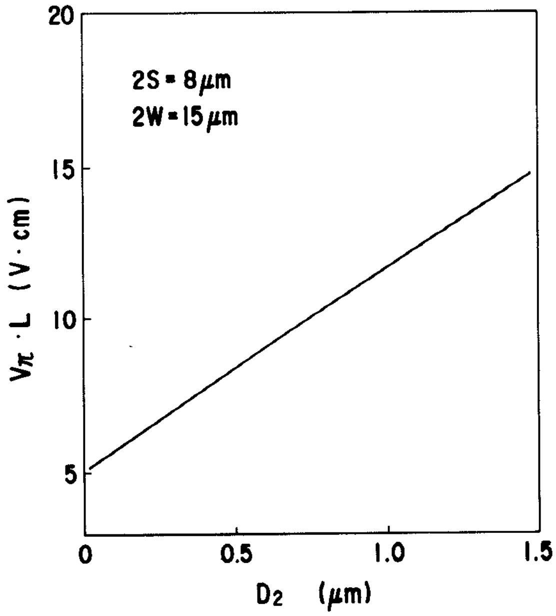

Fig. 7. Calculated value of the product ($V_\pi \cdot L$) of half-wavelength voltage (V_π) and interaction length (L) between microwaves and optical waves.

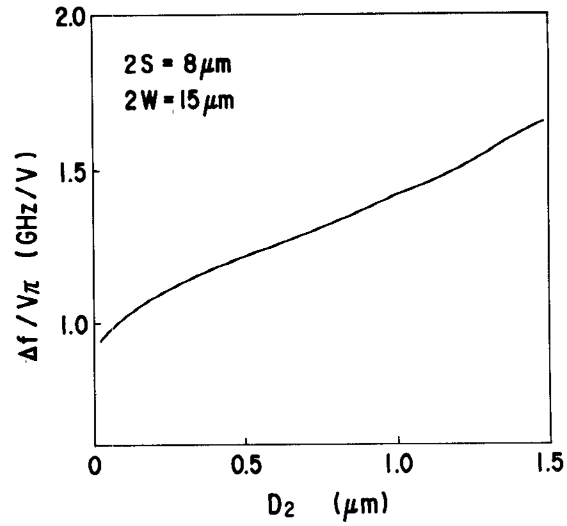

Fig. 8. Calculated results for the figure of merit ratio ($\Delta f / V_\pi$) of modulation bandwidth (Δf) and half-wavelength voltage (V_π) as a function of buffer layer thickness (D_2). Interaction length was assumed to be 2.7 cm. Velocity mismatch, impedance mismatch, and microwave conductor loss were taken into consideration.

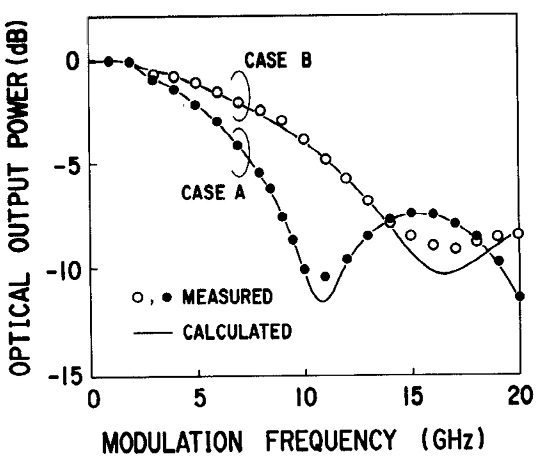

Fig. 9. Calculated and measured optical output power as a function of modulation frequency. Case A has a relatively thick buffer layer of 0.45 μm. Case B has a thick buffer layer of 1.2 μm.

V. Experimental Results

Mach–Zehnder intensity modulators were actually fabricated at a 1.52 μm wavelength. The fabrication conditions for the optical waveguide and the CPW TW electrode were the same as those in [3], [4] except for a Ti film thickness of 800 Å and the wet-O_2 Ti diffusion conditions. The electrode thickness was 4 μm. In order to investigate the validity of the previously mentioned analytical methods, two values for the buffer layer thicknesses (D_2), 0.45 μm and 1.2 μm, were examined.

Fig. 9 shows calculated and measured optical output power as a function of the modulation frequency. The oscillation wavelength of the laser diode module was 1.52 μm. Case A has a relatively thick buffer layer of 0.45 μm [3], [4], a center conductor width of 8 μm, a gap of 30 μm, and an interaction length of 2 cm. Case B has a thick buffer layer of 1.2 μm, a center conductor width of 8 μm, a gap of 15 μm, and an interaction length of 2.7 cm. The interaction lengths for cases A and B were determined so as to obtain driving voltages of less than 5 V. The calculated results for the effective index (n_m) and the characteristic impedance (Z) were 3.54 and 60 Ω for case A and 2.82 and 62.8 Ω for case B, respectively. Although the electrode thickness was assumed to be zero in this analysis, the thickness (4 μm) was small in comparison with gap (15 μm) in the experiment. Thus, good agreement between the calculated and the measured modulation characteristics was obtained. The optical 3 dB bandwidths for the optical modulators in case A and case B were 6.2 GHz and 8.7 GHz. Furthermore, the measured driving voltages were in good agreement with the calculated results for both case A (4.4 V) and case B (4.9 V).

This good agreement of both the modulation bandwidths and the driving voltages verifies the validity of the analytical methods. The optical insertion loss and extinction ratio of the Mach–Zehnder optical modulators for both cases A and B were 2.2 dB and 25 dB.

VI. Conclusion

Analytical methods and results for Mach–Zehnder optical modulators have been described from the viewpoint of CPW TW electrode design. The analyses were based on quasi-TEM and hybrid-mode SDA with the anisotropic effect incorporated. The microwave effective index, the characteristic impedance, and conductor losses were taken into consideration to accurately model modulator characteristics.

It has been confirmed that the SiO_2 buffer layer plays a very important role in both the modulation bandwidth and the half-wavelength voltage. Agreement between the calculated and experimental results for both the modulation characteristics and the driving voltage was quite good. Furthermore, z-cut $LiNbO_3$ Mach–Zehnder optical modulators of wide bandwidths with about 9 GHz and low driving voltages of less than 5 V at a 1.52 μm wavelength have been realized.

Acknowledgment

The authors would like to express their appreciation to Dr. T. Ikegami and Dr. T. Sugeta for their stimulating discussions and encouragement. They also wish to thank O. Mitomi and H. Miyazawa for their fruitful discussions.

References

[1] S. K. Korotoky *et al.*, "4-Gb/s transmission experiment over 117 km of optical fiber using a Ti:LiNbO3 external modulator," *J. Lightwave Technol.*, vol. LT-3, pp. 1027–1031, 1985.

[2] K. Hagimoto, Y. Miyamoto, T. Kataoka, K. Kawano, and M. Ohata, "A 17 Gb/s long-span fiber transmission experiment using a low-noise broadband receiver with optical amplification and equalization," in *Tech. Dig., Optical Amplifiers and Their Applications* (Monterey, CA), 1990, paper TuA2.

[3] K. Kawano, T. Kitoh, O. Mitomi, T. Nozawa, and H. Jumonji, "High-speed and low driving power Ti:$LiNbO_3$ Mach–Zehnder optical modulator at 1.5 μm wavelength," in *Proc. IEEE LEOS Annual Meeting* (Lasers and Electro-Optics Society), 1988, paper OE6.5.

[4] K. Kawano, T. Kitoh, O. Mitomi, T. Nozawa, and H. Jumonji, "A wide-band and low-driving-power phase modulator employing a Ti:$LiNbO_3$ optical waveguide at 1.5 μm wavelength," *IEEE Photonic Technol. Lett.*, vol. 1, pp. 33–34, 1989.

[5] D. Marcuse, "Electrostatic field of coplanarlines computed with the point matching method," *J. Lightwave Technol.*, vol. 7, pp. 939–947, 1989.

[6] Y. Fukuoka, Y. H. Shih, and T. Itoh, "Analysis of slow-wave coplanar waveguide for monolithic integrated circuits," *IEEE Trans. Microwave Theory Tech.*, vol. MTT-31, pp. 567–573, 1983.

[7] Y. Hayashi and R. Mittra, "An analytical investigation of finlines with magnetized ferrite substrate," *IEEE Trans. Microwave Theory Tech.*, vol. MTT-31, pp. 495–498, 1983.

[8] M. Izutsu *et al.*, "Millimeter-wave light modulator using $LiNbO_3$ waveguide with resonant electrode," in *Tech. Dig., Conf. Lasers and Electro-Optics* (Optical Society of America), 1988, paper 14-1.

[9] K. Kubota, J. Noda, and O. Mikami, "Traveling wave optical modulator using a directional coupler $LiNbO_3$ waveguide," *IEEE J. Quantum Electron.*, vol. QE-16, pp. 754–760, 1980.

[10] S. H. Lin and S. Y. Wang, "High throughput GaAs p-i-n electrooptic modulator with a 3-dB bandwidth of 9.6 GHz at 1.3 μm," *Appl. Opt.*, vol. 26, pp. 1696–1700, 1987.

[11] E. J. Denlinger, "Losses of microstrip lines," *IEEE Trans. Microwave Theory Tech.*, vol. MTT-28, pp. 513–522, 1980.

[12] C. P. Wen, "Coplanar waveguide: Surface strip transmission line suitable for nonreciprocal gyromagnetic device applications," *IEEE Trans. Microwave Theory Tech.*, vol. MTT-17, pp. 1087–1090, 1969.

[13] N. J. Parsons, A. C. O'Donnello, and K. K. Wong, "Design of efficient and wideband traveling-wave modulators," in *SPIE*, vol. 651, *Integ. Opt. Cir. ENG. III*, (Insbruck), 1986, paper 24.

[14] M. Seino, N. Mekada, T. Namiki, and H. Nakajima, "33-GHz·cm broadband Ti:LiNbO3 Mach-Zehnder modulator," in *Proc. ECOC* (Gothenburg), 1989, paper ThB22-5.

[15] K. Kawano, T. Nozawa, M. Yanagibashi, and H. Jumonji, "Broadband and low-driving-power $LiNbO_3$ external optical modulators," *NTT Review*, vol. 1, pp. 103–113, 1989.

[16] K. Kawano, T. Kitoh, H. Jumonji, T. Nozawa, and M. Yanagibashi, "New travelling-wave electrode Mach–Zehnder optical modulator with 20 GHz bandwidth and 4.7 V driving voltage at 1.52 μm wavelength," *IEE Electron. Lett.*, vol. 25, pp. 1382–1383, 1989.

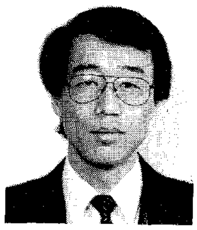

Kenji Kawano received the B.S. and M.S. degrees in physics and applied physics from Kyushyu University, Fukuoka, Japan, in 1977 and 1979, respectively. He received the Ph.D. degree in 1989.

He joined the Musashino Electrical Communication Laboratory, Nippon Telegraph and Telephone (NTT) Corporation, Tokyo, Japan, in 1979, and was engaged in research on thin-film waveguides for microwave integrated circuits. Since 1982, his major efforts have been directed toward the research and development of optical devices for single-mode fibers, with emphasis on problems of semiconductor-laser-to-fiber coupling. Recently, his interest has been focused on the design and fabrication of high-speed $LiNbO_3$ optical waveguide modulators and multiple-quantum-well (MQW) semiconductor optical modulators. He is an author of a book on coupling systems (*Introduction and Application of Optical Coupling Systems for Optical Devices*, Tokyo, Gendai Kougakushya, 1991). He is now a senior research engineer, supervisor, at the NTT Optoelectronics Laboratories.

Dr. Kawano is a member of the Institute of Electronics and Communication Engineers of Japan.

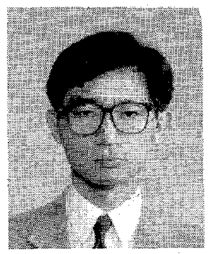

Tsutomu Kitoh was born in Nagoya, Japan, on November 23, 1960. He received the B.S. and M.S. degrees in electrical engineering from Nagoya University, Nagoya, in 1983 and 1985, respectively.

In 1985, he joined the Musashino Electrical Communications Laboratories, Nippon Telegraph and Telephone Corporation (NTT), Musashino, Japan. He has been engaged in research on optical modulators.

Mr. Kotoh is a member of the Institute of Electronics, Information and Communication Engineers of Japan and the Japan Society of Applied Physics.

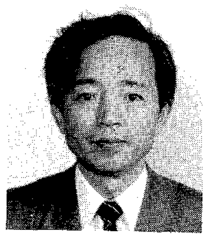

Hiromichi Jumonji was born on January 5, 1940. He received the B.S. degree in electrical engineering from Nihon University, Tokyo, Japan, in 1968 and received the Ph.D. degree in engineering from the University of Tokyo in 1978.

From 1968 to 1974, he was with the Institute of Industrial Science, University of Tokyo, where he did research on monolithic crystal filters and electromechanical functional devices. In 1974, he joined the Electrical communication Laboratories Nippon Telegraph and Telephone Public

Corporation (NTT), where his research and development efforts were concentrated on high-reliability electrical circuit components, hybrid integrated circuits, and cesium atomic clock supply for transmission and switching systems. He recently supervised the development of optical circuit components and $LiNbO_3$ optical devices for optical communication systems. Since April 1990 he has been General Manager of the Optical Research Center at the Research and Development Center, Ricoh Company Ltd., Yokohama.

Dr. Jumonji is a member of the Institute of Electronics and Communication Engineers of Japan and the Japan Society of Applied Physics.

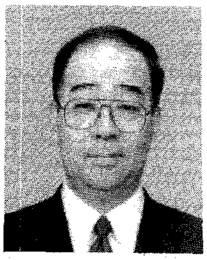

Toshinori Nozawa received the B.S. degree in electronic engineering from Ibaraki University, Japan, in 1969.

He joined the Electrical Communications Laboratories, Nippon Telegraph and Telephone Corporation (NTT), in 1969. Since then he has been engaged in developmental research on $BaTiO_3$ ceramic dielectrics, full wafer LSI's, thin-film devices using ZrN films and a-Si films, and other electronic devices. Since 1986, his major efforts have been directed toward developmental research on high-speed guided-wave optical modulators and switches employing $LiNbO_3$. Since July 1990, he has been engaged in R&D public relations. He is now Senior Engineer, Supervisor, at the NTT R&D Information, Patent and Licensing Center.

Mr. Nozawa is a member of the Institute of Electronics, Information and Communication Engineers in Japan and of the Japan Society of Applied Physics.

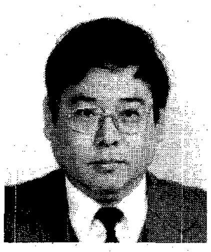

Mitsuaki Yanagibashi was born in 1948.

He joined the Musashino Electrical Communication Laboratory, Nippon Telegraph and Telephone Public Corporation, Tokyo, Japan, in 1967. He has been engaged in the reliability engineering of transistors and aluminum electrolytic capacitors. He has also been working on the reliability of optical components.

Mr. Yanagibashi is a member of the Institute of Electronics and Communication Engineers of Japan.

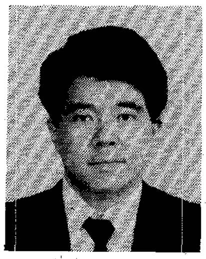

Toshio Suzuki received the B.E. degree in electronic engineering from Tokyo Denki University, Japan, in 1969.

He joined the Electrical Communication Laboratories, NTT, in 1965. Since then he has been engaged in developmental research on plastic insulating materials, piezoelectric plastics, ferrites, and Si single crystals. He is presently engaged in work on thin-film resistors.

Mr. Suzuki is a member of the Institute of Electronics and Communication Engineers of Japan and the Japan Society of Applied Physics.